

01 Sep 1975

## Two-Point, Two Component, Velocity Measurements in Turbulent Pipe Flow

J. S. Cintra Jr.

B. G. Jones

Follow this and additional works at: <https://scholarsmine.mst.edu/sotil>

 Part of the [Chemical Engineering Commons](#)

---

### Recommended Citation

Cintra, J. S. Jr. and Jones, B. G., "Two-Point, Two Component, Velocity Measurements in Turbulent Pipe Flow" (1975). *Symposia on Turbulence in Liquids*. 7.  
<https://scholarsmine.mst.edu/sotil/7>

This Article - Conference proceedings is brought to you for free and open access by Scholars' Mine. It has been accepted for inclusion in Symposia on Turbulence in Liquids by an authorized administrator of Scholars' Mine. This work is protected by U. S. Copyright Law. Unauthorized use including reproduction for redistribution requires the permission of the copyright holder. For more information, please contact [scholarsmine@mst.edu](mailto:scholarsmine@mst.edu).

## TWO-POINT, TWO-COMPONENT, VELOCITY MEASUREMENTS IN TURBULENT PIPE FLOW

J. S. Cintra, Jr. and B. G. Jones  
University of Illinois at Urbana-Champaign

### ABSTRACT

An experimental study of the turbulent velocity field structure was performed in a pipe flow. The primary objective of this study was to provide a detailed velocity field structure, under isothermal conditions, for use as a reference condition for later investigations of the interactions between fluctuating velocity and temperature fields, under non-isothermal conditions, in turbulent pipe flow.

Two-point, two-component ( $u_1$  and  $u_2$ ) velocity correlation measurements were made with hot-film ('x' probes) anemometers separated in the radial direction as well as two-point axial component correlation measurements with axial separation.

The fluctuating signals were analyzed digitally and both space and space-time correlations were calculated.

Spatial scales for each velocity component were determined and then used in the modeling of two-point space correlations in terms of axisymmetric tensor forms. Finally isocorrelation curves were evaluated from the axisymmetric models to test their prediction capabilities.

### INTRODUCTION

Confined turbulent flows are of prime interest in engineering applications.

Due to the random nature of the physical quantities which describe these flows, e.g. velocity, pressure, temperature etc., they can commonly be analyzed in terms of their statistical properties. It is currently impractical to obtain explicit analytical descriptions of velocity, temperature or pressure fluctuating fields. All theories of turbulence, both analytical and semi-empirical, were constructed based on statistical properties of these random quantities. The present experimental research is concerned with semi-empirical theories based on "eddy diffusivity" concepts. Although the treatment given to the turbulence phenomena in these models may appear oversimplified, they are still extremely useful in many practical applications, e.g. the evaluation of momentum (or heat) transfer in a confined steady state turbulent shear flow. In many of

these theories, e.g. Prandtl's (1925) mixing length hypothesis, Von Karman's (1930) similarity hypothesis (see H. Schlichting (1968)), Taylor's (1932) vorticity transport theory, and more recently, Jenkins (1951), Azer & Chao (1960) and Kudva *et al.* (1968), simplifications are made on the governing equations by introducing eddy diffusivities determined from length scales and characteristic velocities. These characterizing quantities are expected to be related to the geometry of the problem and the type of flow and are usually obtained experimentally.

In these previous models only "spherical eddies" are considered and therefore they require the specification of only one length scale. The model for eddy diffusivities proposed initially by Tyldesley and Silver (1968) and with more details by Silver (1968) and Tyldesley (1969, 1970) can allow the eddies to deviate from a spherical shape. Therefore, it requires, at least, a two-parameter representation of the eddies which can be obtained directly from experimental iso-correlation plots, i.e., by cross correlating two-point signals. Although always possible, this approach may require an excessive number of data points to become useful. If some simplifying assumptions are made with respect to the properties of the two-point correlation tensor, it is then possible to reduce the amount of experimentation needed and take two-point measurements only along some appropriate directions in the flow field. Isotropy and axisymmetry are two possible simplifying assumptions for structural forms for turbulence. In the present work the prediction capabilities of the axisymmetric forms are explored in connection with two-point measurements along two orthogonal axes in the flow field. The need to make these measurements is due to the unsatisfactory status of the reported two-point experimental results for turbulent flow in circular pipes. Some length scales from two-point measurements in water, but only for the axial velocity component, are given by Howard (1974), in the flow direction, and by Meek (1972), in the transverse direction. In air some results for the normal component of the velocity are given by Sabot *et al.* (1973), but only at one radial location.

Therefore the primary objective of this study is modeling two-point velocity correlations in pipe flow. The purpose is to provide a basis for a later investigation into the Tyldesley and Silver (1968) eddy diffusivity model. The experimental input needed for the correlation modeling is obtained in terms of length scales for two fluctuating velocity components ( $u_1$  and

$u_2$ ) along two orthogonal directions (parallel (axial) and normal (radial) to the mean flow). Three scales are measured directly from space-correlations and a fourth one is estimated. Two axisymmetric models are investigated, namely, the two-parameter model proposed by Goldstein and Rosenbaum (1973) and the four parameter model suggested by Weber (1974).

#### EXPERIMENT DESCRIPTION

All measurements reported here were carried out in the heat transfer loop described in detail by Burchill (1970). The test section is vertical, has a circular cross section with an inside diameter of 4.01 in. and is 28 ft. long. In Figure 1 is shown

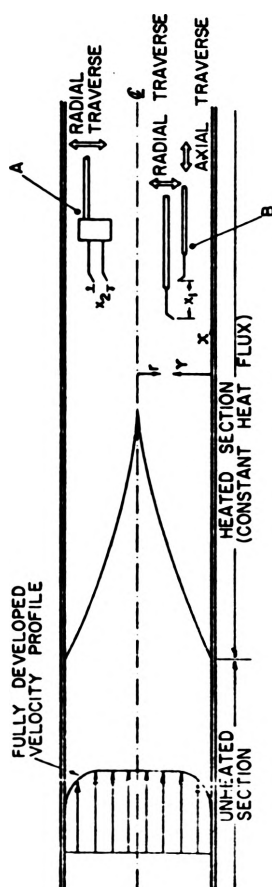


Figure 1 - Test section illustrating relative probe positions  
A - radial separation measurements  
B - axial separation measurements

schematically the upper portion of the test section illustrating relative probe positions for both radial and axial separation measurements. A traversing mechanism, designed to enter the test section from the top, allowed radial traverse as well as axial positioning.

The fluctuating velocity signals were taken under isothermal conditions at a section 79.5 diameters from

the test section entrance. Burchill (1970) using axial pressure drop and turbulent shear data showed that fully developed flow conditions were established at that location. The fluid used in those experiments was demineralized water to allow the use of uncoated hot-film anemometer sensors.

For the two-point, two-component velocity measurements two end flow 'x' probes were used, thus requiring four channels of anemometry. Each channel of anemometry was made up of one DISA type 55D01 Anemometer, one DISA type 55D10 Linearizer, one BAY LAB Model 5123 DC amplifier used as a Low Pass filter (-18 dB/octave) with a -3db setting at 1 KHz, and one TSI Model 1015C Correlator used for AC coupling with cutoff frequency set at 0.1 Hz (-12dB/octave). The four filtered signals were then recorded on magnetic tape on a SANGAMO Model 3564 FM Tape Recorder.

The fluctuating signals were analyzed, on playback, with a TSI 1065A (≡ Honeywell-Saicor Model 42) Digital Correlation and Probability Analyzer. In order to separate the axial from the normal component of the velocity, in the case of 'x' probe signals, two TSI 1015C Sum and Difference Correlators were used between the tape recorder and the 1065A. By an appropriate adjustment of the input gains in the 1015C and by operating it on the sum (or difference) mode we can generate an output signal proportional to the  $u_1$  (or  $u_2$ ) component of the fluctuating velocity at one point. The same procedure can be applied to the 'x' probe placed at the other point. The 1065A, after sampling and digitizing the input signals, produced auto and cross-covariances as functions of delay time which were plotted on a Houston Model 2000 X-Y Plotter. In addition to that output the zero lag time and the peak values were read on a Hewlett-Packard Model 34702A Digital Multimeter.

The cross-covariances, normalized with the square roots of the zero delay time auto-covariances, generated the correlation functions shown in Figures 2 and 3.

For the axial separation, axial component, velocity measurements a radial offsetting procedure was used to minimize interference effects on the signal from the downstream probe and correction factors were applied to the small separation correlation functions in Figure 3. A correction factor was determined for each axial separation by plotting the correlation coefficients vs. radial separation and selecting the operating condition at the smallest separation where these coefficients show no significant effect of the wake of the upstream sensor.

More details concerning instrumentation and techniques involved in these measurements are given by Cintra (1975).

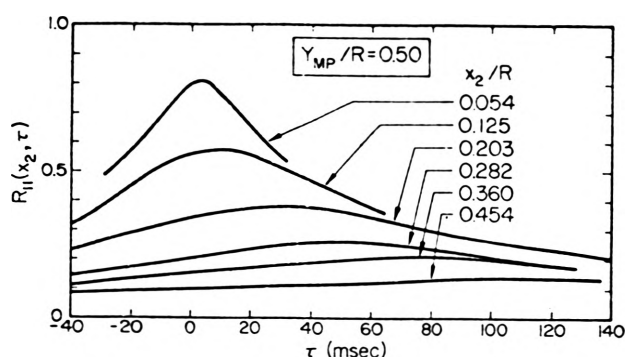


Figure 2 - Space-time correlations - axial velocity component, transverse separations

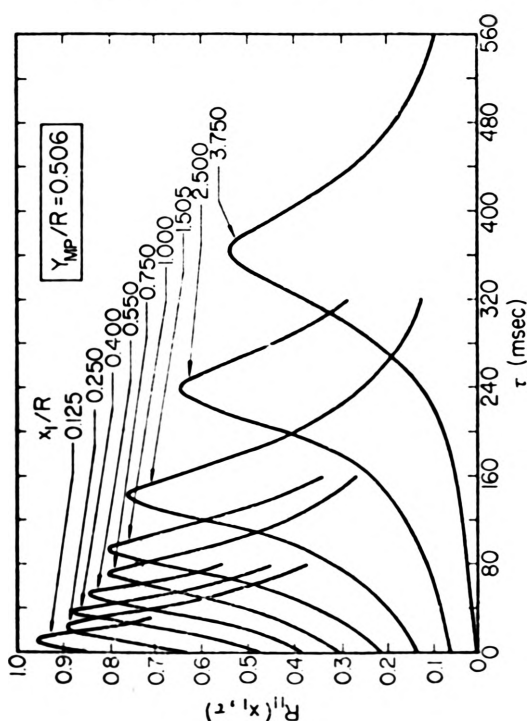


Figure 3 - Space-time correlations - axial velocity component, axial separations

#### VELOCITY FIELD RESULTS

Following the procedures previously outlined two groups of measurements were made, namely, two-point transverse separation measurements with x-probes and two-point axial separation single-sensor measurements. For all runs the flow rate was set such as to give a pipe Reynolds number of 56,590 and the bulk water temperature was kept approximately constant, with a deviation of the average of less than  $0.6^\circ\text{F}$ , and equal to  $80^\circ\text{F}$ .

Measurements were taken and the fluctuating signals processed at several radial locations (5 for transverse,  $x_2$ , separation measurements and 4 for axial,

$x_1$ , separation measurements). However, not all the results obtained will be presented and only one radial location will be considered in the two-point correlation modeling.

In Figures 2 and 3 are presented space-time correlations for the axial component of the velocity obtained, respectively, from transverse and axial separation measurements. The interpretation of space-time curves from measurements with separations in the flow direction has become common in terms of a convected frame structure. However, little attention has been paid so far to similar measurements with separations in a direction normal to the mean flow. It will be shown later in this paper that such measurements may be extremely useful in modeling two-point correlations and estimating shapes of the turbulent eddies.

In Figure 4 are presented space-correlation results for the normal velocity component from  $x_2$  separation measurements. A similar set of results was obtained for the axial velocity component. Both sets were then used to calculate the integral length scales shown in Figure 5. In this figure a trend toward equal scales for velocity components is observed as one moves away

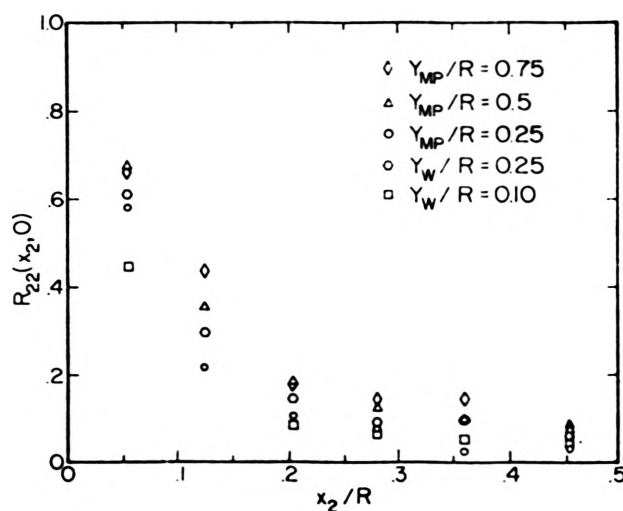


Figure 4 - Space correlations - normal velocity component, transverse separations

from the wall and in the direction of the center of the pipe. The same trend was also observed with length scales for temperature fluctuations (reported by Cintra (1975)), where  $L_{22}^{(2)} < L_{tt}^{(2)} < L_{11}^{(2)}$  was obtained for all measured radial locations.

Integral time-scales in the convected frame for the axial component of the velocity were calculated by an exponential fit to the envelope of all space-time curves with axial separation (Figure 2). These results are presented in Table 1 together with estimated values for the time scale for the normal component of the velocity obtained by using the ratios between these scales reported by Sabot and Comte-Bellot (1974). Finally, integral length scales for the normal component of the velocity calculated with

$$L_{22}^{(1)} = T_{22}^{(1)} u_2^1 \quad (1)$$

are also given in Table 1.

y/R	$T_{11}^{(1)}$	$T_{22}^{(1)}(\text{est})$	$L_{22}^{(1)}(\text{est})$
	(msec)	(msec)	(in)
0.75	668	227	0.164
0.50	585	133	0.112
0.25	560	88	0.086
0.10	358	43	0.046

Table 1 - Integral time and length scales

#### AXISYMMETRIC MODELING OF TWO-POINT CORRELATIONS

The inappropriateness of the isotropic models to represent confined shear flows can readily be seen by looking at the differences between the intensities for the various velocity components or the existence of non-zero shear coefficients. Therefore, to represent two-point correlations we have examined somewhat more complicated forms; namely, the ones from axisymmetric models.

The theory of axisymmetric turbulence was first derived by Batchelor (1946) and extended by Chandrasekhar (1950). In this theory the two-point correla-

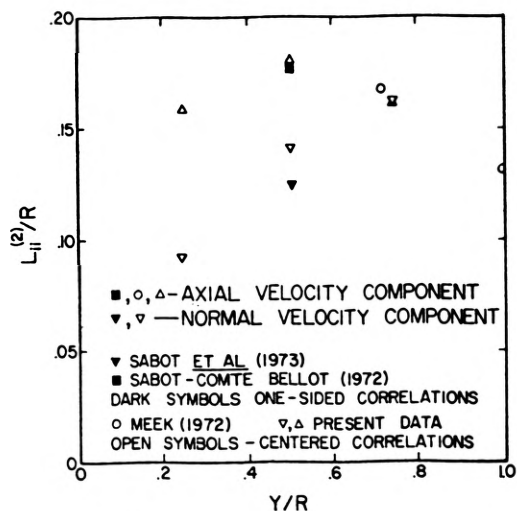


Figure 5 - Integral length scales transverse direction  
Centered correlations

$$L_{ii}^{(2)}(Y_W) = \int_0^{x_2^0} R_{ii} \left[ \left| Y - \frac{x_2}{2} \right|, \left| Y + \frac{x_2}{2} \right| \right] dx_2$$

One-sided correlations

$$L_{ii}^{(2)}(Y_W) = \int_0^{x_2^0} R_{ii} \left[ (Y), (Y + x_2) \right] dx_2$$

with  $x_2^0$  = first zero crossing

tion tensor defined by

$$Q_{ij} = \overline{u_i(\vec{x}) u_j(\vec{x} + \vec{x})} \quad (2)$$

is invariant only for rotations with respect to a preferred axis ( $\vec{\lambda}$ ) and reflections in planes containing this axis. This theory assumes homogeneity which makes it applicable only to regions in the flow field where the length scales are small compared to the spatial variation of the turbulence intensities. The end result of this theory is that the correlation tensor  $Q_{ij}$  can be fully represented by knowledge of two-scalar functions  $Q_1$  and  $Q_2$  of the variables  $r^2$  and  $r\mu$  such that the following equations are satisfied (Chandrasekhar 1950)

$$Q_{ij} = A \xi_i \xi_j + B \delta_{ij} + C \lambda_i \lambda_j + D (\lambda_i \xi_j + \xi_i \lambda_j) \quad (3)$$

where

$$A = (D_r - D_{\mu\mu}) Q_1 + D_r Q_2 \quad (4a)$$

$$B = [-(r^2 D_r + r\mu D_{\mu} + 2) + r^2 (1 - \mu^2) D_{\mu\mu} - r\mu D_{\mu}] Q_1 - [r^2 (1 - \mu^2) D_r + 1] Q_2 \quad (4b)$$

$$C = -r^2 D_{\mu\mu} Q_1 + (r^2 D_r + 1) Q_2 \quad (4c)$$

$$D = (r\mu D_\mu + 1) D_\mu Q_1 - \mu r D_r Q_2 \quad (4d)$$

with  $r^2 = \vec{\xi} \cdot \vec{\xi}$ ,  $r\mu = \vec{\xi} \cdot \vec{\lambda}$  (as shown in Fig. 6),

$$D_r = \frac{1}{r} \frac{\partial}{\partial r} - \frac{\mu}{r^2} \frac{\partial}{\partial \mu}, \quad D_\mu = \frac{1}{r} \frac{\partial}{\partial \mu} \quad \text{and} \quad D_{\mu\mu} = D_\mu D_\mu$$

In order to relate correlations with the scalar functions  $Q_1$  and  $Q_2$  let us consider the systems of coordinates shown in Figure 6.

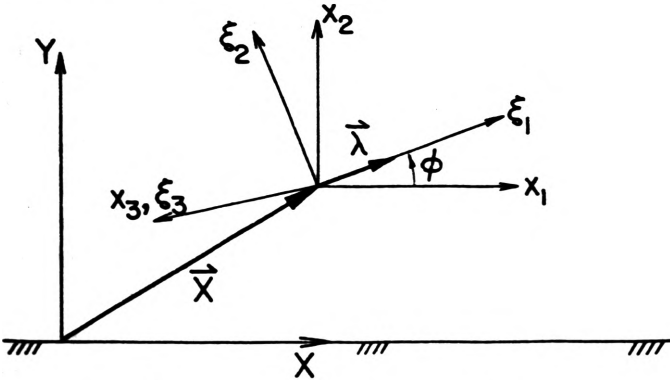


Figure 6 - Systems of separation coordinates  
( $x_1, x_2, x_3$ ) - measurement system  
( $\xi_1, \xi_2, \xi_3$ ) - axisymmetric system

If we use a tilde to represent components of vectors and tensors in the axisymmetric system of coordinates, we have relations between correlations in the two systems of the form

$$R_{11}(x_1, x_2, x_3) = \tilde{R}_{11}(\xi_1, \xi_2, \xi_3) \cos^2 \phi - 2\tilde{R}_{12}(\xi_1, \xi_2, \xi_3) \cdot \sin \phi \cos \phi + \tilde{R}_{22}(\xi_1, \xi_2, \xi_3) \sin^2 \phi \quad (5)$$

where  $\tilde{R}_{11}$ ,  $\tilde{R}_{12}$  and  $\tilde{R}_{22}$  are given by the following differential equations (Goldstein & Rosenbaum - 1973)

$$\tilde{R}_{11} = -\frac{1}{\sigma} \frac{\partial}{\partial \sigma} \left[ \sigma^2 \frac{Q_1(\xi_1, \sigma)}{u_1^2} \right] \quad (6)$$

$$\begin{aligned} \tilde{R}_{22} = & -\frac{\partial}{\partial \xi_3} \left[ \xi_3 \frac{Q_2(\xi_1, \sigma)}{u_2^2} \right] + \\ & + \left( \xi_3^2 \frac{\partial^2}{\partial \xi_1^2} - \frac{2\sigma^2}{\partial \xi_1 \partial \xi_2} + \xi_1^2 \frac{\partial^2}{\partial \xi_3^2} \right) \frac{Q_1(\xi_1, \sigma)}{u_2^2} \end{aligned} \quad (7)$$

$$\tilde{R}_{12} = \frac{\partial}{\partial \xi_1} \left[ \frac{Q_1(\xi_1, \sigma)}{u_1^2} \right] \quad (8)$$

$$\text{with } \sigma^2 = \xi_2^2 + \xi_3^2 \quad (9)$$

The remaining problem to obtain a representation of the two-point correlations is the specification of the scalar functions  $Q_1$  and  $Q_2$ . Two approaches were analyzed: the two-parameter model from Goldstein & Rosenbaum (1973) and the four parameter model from Weber (1974).

Goldstein & Rosenbaum (1973) have proposed the following relations for the defining scalars  $Q_1$  and  $Q_2$

$$Q_1(\xi_1, \sigma) = -\frac{\bar{u}_1^2}{2} \exp \left[ -\sqrt{\left( \frac{\xi_1}{\ell_1} \right)^2 + \left( \frac{\sigma}{\ell_2} \right)^2} \right] \quad (10)$$

$$Q_2(\xi_1, \sigma) = -(\bar{u}_2^2 - \bar{u}_1^2) \exp \left[ -\sqrt{\left( \frac{\xi_1}{\ell_1} \right)^2 + \left( \frac{\sigma}{\ell_2} \right)^2} \right] \quad (11)$$

By using (10) and (11) we can solve (6) through (8) and then use relations like (5) to obtain expressions for the correlations in the flow system of coordinates. Finally, by integration, we can use measured experimental length scales to evaluate the parameters  $\ell_1$  and  $\ell_2$ , e.g., through

$$L_{11}^{(2)} = \int_0^{x_{20}} R_{11}(0, x_2, 0) dx_2 \quad (12)$$

with  $x_{20}$  = first zero crossing of  $R_{11}(0, x_2, 0)$ .

From this we obtain

$$\left( \frac{\ell_1}{\ell_2} \right)^2 = \frac{2 \sin^2 \phi \left\{ \left( \frac{\bar{u}_2^2}{\bar{u}_1^2} - 1 \right) [(\rho+1) \cos^2 \phi - 1] + \rho \right\}}{1 - 2 \cos^2 \phi \left\{ \left( \frac{\bar{u}_2^2}{\bar{u}_1^2} - 1 \right) [(\rho+1) \cos^2 \phi - 1] + \rho \right\}} \quad (13)$$

and

$$\ell_1 = \frac{\bar{u}_1^2 L_{22}^{(2)} (\sin^2 \phi + \rho_1^2 \cos^2 \phi)^{1/2}}{\bar{u}_1^2 \sin^2 \phi + \bar{u}_2^2 \cos^2 \phi} \quad (14)$$

with

$$\rho = \frac{\bar{u}_1^2 L_{11}^{(2)}}{\bar{u}_2^2 L_{22}^{(2)}}, \quad \rho_1 = \frac{\ell_1}{\ell_2} \quad (15)$$

The first difficulty in using this two parameter model is that for a given set of length scales the allowed angles of axisymmetry may not yield realistic correlation functions. For example, for pipe flow and from measurements at  $Y/R = 0.50$  the solutions of (13) (presented in Figure 7), it is clear that only values for the angle of axisymmetry close to  $90^\circ$  are allowed. If we use some  $\phi$  angle in this range the resultant

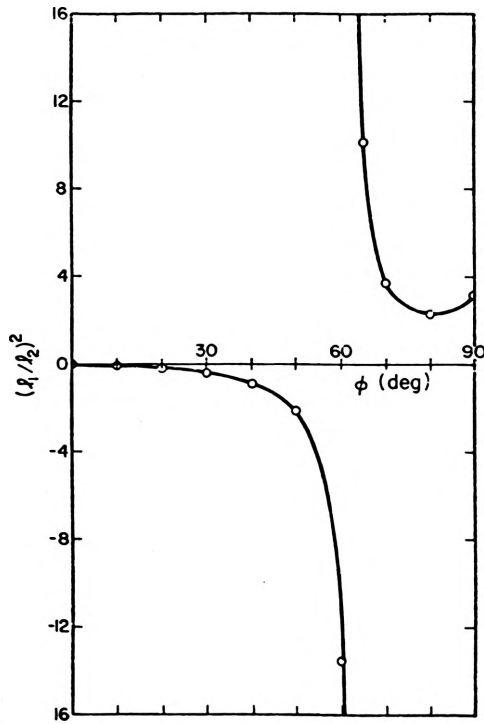


Figure 7 - Angular dependence of free parameter ratio in Goldstein model with  $L_{11}^{(2)}/L_{22}^{(2)} = 1.276$  isocorrelation contours (shown in Figure 8) are unacceptable for pipe flow (Sabot-Comte Bellot - 1972).

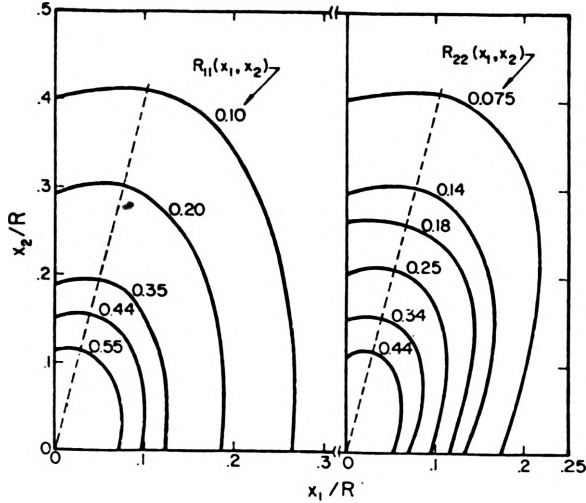


Figure 8 - Isocorrelation contours - Goldstein two parameter model

A similar analysis can be applied by using other measured values of length scales, e.g.  $L_{11}^{(1)}$  and  $L_{11}^{(2)}$ . The range of  $\phi$  angles for which solution is possible will be different but the end result still will be that we cannot, for pipe flow, represent well and simultaneously the two correlation functions  $R_{11}(x_1, x_2)$  and  $R_{22}(x_1, x_2)$  with only two free parameters  $l_1$  and  $l_2$ .

This fact led Weber (1974) to derive a four parameter axisymmetric model. However, instead of postu-

lating functional relations for the scalar functions  $Q_1$  and  $Q_2$  depending on four parameters he examined the behaviour of the correlation functions themselves and proposed the following expressions to represent them (letting  $\xi_3 = 0$ , for simplicity, then  $\sigma = \xi_2$ ).

$$\hat{R}_{11}(\xi_1, \xi_2) = \left[ 1 - \frac{1}{2} \frac{\xi_2^2}{l_2^2 \sqrt{\left(\frac{\xi_1}{l_1}\right)^2 + \left(\frac{\xi_2}{l_2}\right)^2}} \right] \exp \left[ -\sqrt{\left(\frac{\xi_1}{l_1}\right)^2 + \left(\frac{\xi_2}{l_2}\right)^2} \right] \quad (16)$$

$$\hat{R}_{22}(\xi_1, \xi_2) = \left[ 1 - \frac{1}{2} \sqrt{\left(\frac{\xi_1}{n_1}\right)^2 + \left(\frac{\xi_2}{n_2}\right)^2} \frac{\xi_1^2}{\xi_1^2 + \xi_2^2} \right] \exp \left[ -\sqrt{\left(\frac{\xi_1}{n_1}\right)^2 + \left(\frac{\xi_2}{n_2}\right)^2} \right] \quad (17)$$

The equation for  $\hat{R}_{11}$  is the same as the one in the previous model and so is  $Q_1$  but  $Q_2$  was then calculated from the postulated expression for  $\hat{R}_{22}$ .

Following the same procedure as before to relate free parameters to experimentally measured length scales we obtain relations

$$\left\{ \begin{array}{l} \frac{1}{\alpha} \frac{\sqrt{2}}{u_1} A_1 + \frac{1}{\pi} \frac{\sqrt{2}}{u_2} C_1 = \overline{u_1^2} L_{11}^{(1)} \\ \frac{1}{\gamma} \frac{\sqrt{2}}{u_1} B_1 + \frac{1}{\Delta} \frac{\sqrt{2}}{u_2} D_1 = \overline{u_1^2} L_{11}^{(2)} \\ \frac{1}{\alpha} \frac{\sqrt{2}}{u_1} A_2 + \frac{1}{\pi} \frac{\sqrt{2}}{u_2} C_2 = \overline{u_2^2} L_{22}^{(1)} \\ \frac{1}{\gamma} \frac{\sqrt{2}}{u_1} B_2 + \frac{1}{\Delta} \frac{\sqrt{2}}{u_2} D_2 = \overline{u_2^2} L_{22}^{(2)} \end{array} \right. \quad (18a) \quad (18b) \quad (18c) \quad (18d)$$

$$\text{with } \alpha = \left( \frac{\cos^2 \phi}{l_1^2} + \frac{\sin^2 \phi}{l_2^2} \right)^{1/2} \quad (19)$$

$$\gamma = \left( \frac{\sin^2 \phi}{l_1^2} + \frac{\cos^2 \phi}{l_2^2} \right)^{1/2} \quad (20)$$

$$\pi = \left( \frac{\cos^2 \phi}{n_1^2} + \frac{\sin^2 \phi}{n_2^2} \right)^{1/2} \quad (21)$$

$$\Delta = \left( \frac{\sin^2 \phi}{n_1^2} + \frac{\cos^2 \phi}{n_2^2} \right)^{1/2} \quad (22)$$

The coefficients  $C_1, C_2, D_1$  and  $D_2$  are functions of the angle of axisymmetry alone and  $A_1, A_2, B_1$  and  $B_2$  are functions of  $\phi$  and the ratio  $(l_1/l_2)$ . The solutions of (18) were obtained by an interactive scheme and the results for different angles of axisymmetry are presented on Table 2. Unlike the two parameter Goldstein model the four parameter model allows solutions only

$\phi$ (DEG)	$(\ell_1/\ell_2)^2$	$(n_1/n_2)^2$	Remarks
60	No Sol.	No Sol.	} $.1 < \ell_1/\ell_2 < 10$
50	No Sol.	No Sol.	
40	6.20	< 0	
30	0.119	< 0	
20	1.195	< 0	
10	0.112	< 0	
	5.407	0.491	

Table 2 - Angular dependence of free parameter ratios  
4 parameter model ( $y/R = 0.50$ )

for small angles of axisymmetry which means that the axis of axisymmetry is more or less aligned with the mean flow as would be expected for fully developed pipe flow.

Up to this point nothing has been said about the physical specifications of the  $\phi$  angle. Weber (1974) used the shear angle as  $\phi$  and showed good agreement with experimental results for the mixing layer in a round jet. In the present work a different approach was taken; namely, by that of considering the space-time correlation curves available from transverse separation measurements (Figure 2). By assuming that the isocorrelation contours can be represented by ellipses and by taking (Sabot-Comte Bellot (1972))

$$R_{11}(x_1^*, x_2; 0) = R_{11}(0, x_2; \tau_m^*) \quad (23)$$

$$\text{with } x_1^* = \tau_m^* U_{ave} = \tau_m^* \frac{1}{x_2} \int_{-x_2/2}^{+x_2/2} \bar{U}_1(Y+n) dn \quad (24)$$

$$\text{and } \left. \frac{\partial R_{11}}{\partial x_1}(x_1, x_2) \right|_{x_1 = x_1^*} = 0 \quad (25)$$

we can calculate the isocorrelation curves presented in Figure 9. In order to check the validity of this procedure predicted correlations along the x-axis were compared with experimentally measured values (dark symbols in Figure 9). Due to this reasonable agreement, we feel that it is acceptable to equate the  $\phi$  angle to the angle between the major axis of the ellipse and the flow direction. It is clear now in Figure 9 why the shear angle ( $24.1^\circ$  at the location studied) can be used only for small separations in pipe flow. If one wants to represent mainly the large scale structure of the correlation functions, a much smaller angle would be appropriate, e.g.  $10^\circ$ , which is consistent with the previous calculations made for the four parameter model and presented on Table 2. Isocorrelation maps calculated with this angle are shown in Figure 10.

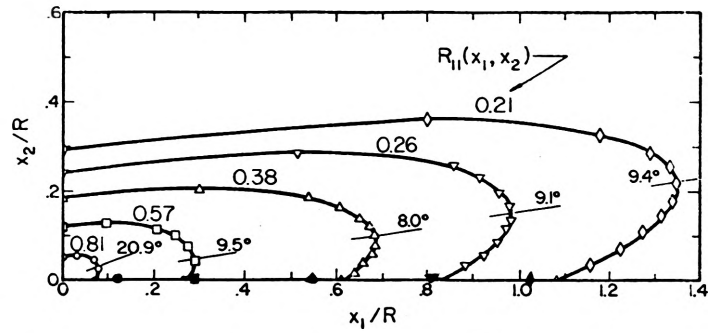


Figure 9 - Ellipse representation of isocorrelation contours

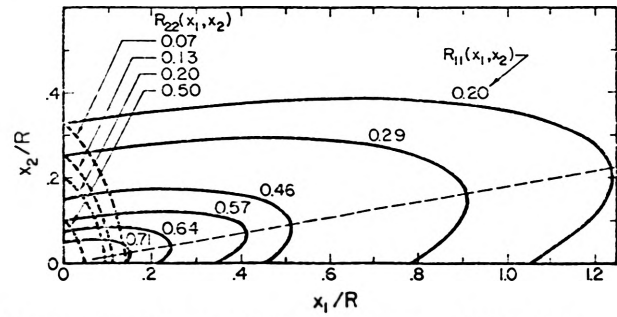


Figure 10 - Isocorrelation contours - Weber four parameter model

#### CONCLUSIONS

The principal conclusions from the measurements made and the two axisymmetric models studied in this work are:

- (1) Space-time cross correlations with transverse separations can be used to estimate the shape of isocorrelated regions in the flow field.
- (2) The main orientation of the isocorrelation contours in pipe flow shows a variable angle of inclination with respect to the mean flow direction.
- (3) The two parameter Goldstein and Rosenbaum (1973) model is not adequate for a two-dimensional representation of the correlation functions for the two components of the fluctuating velocity ( $u_1$  and  $u_2$ ) in pipe shear flow. The four parameter Weber (1974) model can provide a reasonably good description for this type of flow.
- (4) The best value for the angle of axisymmetry to represent large scale eddies in a pipe flow is much smaller than the shear angle.

The following limitations must be added to the previous conclusions:

- (1) The testing of the axisymmetric models in this study was done at only one radial location. The extension of the results and con-

clusions to all other points in the flow field may not be completely valid.

- (2) In both models tested the dependence of the correlation functions on the  $x_3$ -separation coordinate was always combined with the dependence on the  $x_2$ -separation coordinate. As a result  $\gamma_{11}^{(2)} = \gamma_{11}^{(3)}$  was implied in both models, although there is currently no experimental evidence that this holds for pipe flow. Therefore, additional two point measurements in planes of  $x_1 = \text{constant}$  may be in order to further investigate these axisymmetric models.

#### ACKNOWLEDGMENTS

This work was carried out in the Fluid Flow and Heat Transfer Laboratory of the Nuclear Engineering Program of the University of Illinois. Partial support from the University Research Board and the Water Resources Center (B-067-ILL) and the assistance of K. T. Huang in preparing the figures for this paper are gratefully acknowledged.

One of the authors (J.S.C.) is also indebted to the Instituto de Energia Atomica and FAPESP (Brazil) for providing his financial support during his doctoral thesis research of which the present paper is an essential part.

#### LIST OF SYMBOLS

$A, B, C, D$	= defining scalar functions in axisymmetric second order tensor representation
$\ell_1, \ell_2$	= parameters - axisymmetric models
$L_{ii}^{(j)}$	= integral length scale of the $i^{\text{th}}$ velocity component in $j^{\text{th}}$ - direction.
$n_1, n_2$	= parameters - axisymmetric models
$Q_{ij}$	= second order two-point covariance tensor
$Q_1, Q_2$	= defining scalar functions in axisymmetric second order tensor representation
$R$	= pipe radius
$R_{ij}$	= second order two-point correlation tensor
$T_{ii}^{(1)}$	= integral convected time scale of the $i^{\text{th}}$ velocity component
$u_i$	= $i^{\text{th}}$ component of fluctuating fluid velocity
$U_i$	= $i^{\text{th}}$ component of local fluid velocity
$X, Y, Z$	= components of position vector-cartesian system
$x_1, x_2, x_3$	= components of separation vector-measurement system

#### GREEK LETTERS

$\vec{\lambda}$	= vector, defining axis of rotational invariance
$\xi_1, \xi_2, \xi_3$	= components of separation vector-axisymmetric system
$\tau$	= time delay
$\tau_m^*$	= optimum time delay for cross-correlation with transverse separation
$\phi$	= angle of axisymmetry

#### SUPERSCRIPTS

$-$	= denotes long time average
$\sim$	= denotes quantity evaluated in the axisymmetric system of coordinates
$'$	= denotes root mean square of a fluctuating quantity
(i)	= denotes $i^{\text{th}}$ separation direction

#### SUBSCRIPTS

MP	= denotes distance referred to the mid point between sensors
W	= denotes distance referred to the wall sensor
ij	= denotes velocity components

#### REFERENCES

- Azer, N. Z., and Chao, B. T., 1960, "A Mechanism of Turbulent Heat Transfer in Liquid Metals", Int. J. Heat Mass Transfer, 1, 121.
- Batchelor, G. K., 1946, "The Theory of Axisymmetric Turbulence", Proc. Royal Society-A, 186, 480.
- Burchill, W. E., 1970, "Statistical Properties of Velocity and Temperature Fields in Isothermal and Non-isothermal Turbulent Pipe Flow", Ph.D. Thesis, Nuclear Engineering Program, University of Illinois.
- Chandrasekhar, F. R. S., 1950, "The Theory of Axisymmetric Turbulence", Philosophical Transactions of the Royal Society-A, 242, 557.
- Cintra, Jr., J. S., 1975, "Experimental and Modeling Studies of Two-point Velocity and Temperature Fields in Turbulent Pipe Flow", Ph.D. Thesis, Nuclear Engineering Program, University of Illinois.
- Goldstein, M., and Rosenbaum, B., 1973, "Effect of Anisotropic Turbulence on Aerodynamic Noise", J. Acous. Soc., 54, 3, 630.
- Howard, N. M., 1974, "Experimental Measurements of Particle Motion in a Turbulent Pipe Flow", Ph.D. Thesis, Nuclear Engineering Program, University of Illinois.
- Jenkins, R., 1951, "Variations of the Eddy Conductivity with Prandtl Modulus and its Use in the Prediction of Heat Transfer Coefficients", Proc. of the Heat Transfer and Fluid Mechanics Institute, 147, Stanford University Press.
- Karman, T. Von, 1930, "Mechanische Ähnlichkeit und Turbulenz", Nach. Ges. Wiss. Göttingen, Math. Phys., Kl., 58; see also Proc. 3rd. Intern. Congress App.

Mech., Stockholm, Pt. I, 85 (1930).

Kudva et.al., 1968, "Turbulence Scales and Eddy Diffusivities", Paper presented at the Tenth National Heat Transfer Conference, Philadelphia, Pennsylvania, August 11-14.

Meek, C. C., 1972, "Statistical Characterization of Dilute Particulate Suspensions in Turbulent Fluid Fields", Ph.D. Thesis, Nuclear Engineering Program, University of Illinois.

Prandtl, L., 1925, "Bericht über Untersuchungen zur ausgebildeten Turbulenz", Z. angew. Math. u. Mech., 5, 2, 136; see also Proc. 2nd Intern. Congress Appl. Mech., Zurich (1926).

Sabot, J., and Comte Bellot, G., 1972, "Courbes d'iso-correlations spatiales et d'iso-correlations spatio-temporelles relatives aux fluctuations longitudinales de vitesse en conduite lisse circulaire", C. R. Acad. Sci. Paris t.275-Series A, 667; 1974, "Temps de coherence de la fluctuation radiale de vitesse en conduite lisse circulaire", C. R. Acad. Sc. Paris, t. 278, A, 105.

Sabot, J. et.al., 1973, "Space-time Correlations of the Transverse Velocity Fluctuations in Pipe Flow", Phys. Fluids, 16, 9, 1403.

Schlichting, H., 1968, "Boundary Layer Theory", McGraw Hill Co. - New York.

Silver, R. S., 1968, "Reynolds Flux Concept in Heat and Mass Transfer", The Osborne Reynolds Centenary Symposium, University of Manchester, Sept. 1968.

Taylor, G. I., 1932, "The Transport of Vorticity and Heat through Fluids in Turbulent Motion", Proc. Royal Society-London, 135, A, 685.

Tyldesley, J. R., and Silver, R. S., 1968, "The Prediction of the Transport Properties of a Turbulent Fluid", Int. J. Heat Mass Transfer, 11, 1325.

Tyldesley, J. R., 1969, "Transport Phenomena in Free Turbulent Flows", Int. J. Heat Mass Transfer, 12, 489; 1970, "A Theory to Predict the Transport and Relaxation Properties of a Turbulent Fluid", Proc. Royal Soc.-Edinburgh, 68, A, 271.

Weber, D. P., 1974, "Turbulent Velocity Field Structure in a Round Jet and its Relation to Fluctuating Pressure", Ph.D. Thesis, Nuclear Engineering Program, University of Illinois.

## DISCUSSION

W. W. Willmarth, Univ. of Michigan: What is the angle of maximum shear?

Jones: This is similar to the Moor's circle definition of principal axes and maximum shear and in terms of turbulent velocity components is given by

$$\beta = \tan^{-1} \frac{2 \overline{uv}}{\overline{u^2} + \overline{v^2}}$$

Willmarth: What was the frequency response of your complete system?

Jones: The system had a response from essentially D.C. to 1250 Hz with the lower limit established from the anemometry of ~ 0.1 Hz.

Willmarth: Where in the flow are your correlation contours measured? What is meant by axial symmetry? The patterns you showed don't look axisymmetric.

Jones: The correlation contours are measured in fully developed flow at selected radii with probe separations taken from these radii. The picture is that of an inclined elongated spheroid with principal axes inclined to the mean flow by the angle,  $\phi$ , the angle of axisymmetry, which establishes the principal axis about which the elongated spheroid has rotational symmetry.

Victor Goldschmidt, Purdue University: Did you obtain the same structure at all radial positions?

Jones: We observe a consistent angle between larger separation measurements for a selected Y/R. However, we do not have sufficient data to study effects for different Y/R. Although four Y/R values were used in the study complete evaluation of the correlations in all three separations was not done for each radial selection.

R. L. Hummel; University of Toronto: You are using four length parameters. Can you justify these in terms of adjusting what these parameters represent?

Jones: The values  $\ell_1$ ,  $\ell_2$ ,  $m_1$  and  $m_2$  represent structural parameters which are evaluated within model constraints from the two-dimensional turbulent structure length scales and are not adjustable. However, in the two-parameter model given by eq. (10) through (15) it is clear that any two length scales could be selected to define  $\rho$  in eq. (15) which gives the functional relation of the parameter ratio through eq. (13) as

$$\rho_1^2 = f(\phi, \rho, \overline{u_2^2}, \overline{u_1^2}) .$$